

## Effect of heat transfer enhancement and NO<sub>x</sub> emission using Al<sub>2</sub>O<sub>3</sub>/water nanofluid as coolant in CI engine

M Raja<sup>a\*</sup>, R Vijayan<sup>a</sup>, S Suresh<sup>b</sup> & R Vivekananthan<sup>a</sup>

<sup>a</sup>Department of Mechanical Engineering, Government College of Engineering, Salem 636 011, India

<sup>b</sup>Department of Mechanical Engineering, National Institute of Technology, Tiruchirapalli 620 015, India

*Received 10 August 2011; accepted 9 April 2013*

Heat transfer characteristics of Al<sub>2</sub>O<sub>3</sub>/water nanofluids are studied in a shell and tube heat exchanger under laminar flow condition when used as coolant for a single cylinder diesel engine. Nanofluids are prepared using the two-step method with various volume concentrations of 0.5, 1, 1.5 and 2%. The effect of Peclet number and various volume concentrations on heat transfer characteristics and pressure drop is investigated under laminar flow condition. Based on the results, an increase in volume concentration of nanoparticles in the base fluid causes significant enhancement of heat transfer characteristics compared to distilled water. At a Peclet number of about 3000, the enhancement of the overall heat transfer coefficient at 0.5, 1, 1.5 and 2% Al<sub>2</sub>O<sub>3</sub> nanoparticle volume concentration was about 11%, 18%, 23% and 25%, respectively under no load condition. The measured pressure loss with the use of nanofluids is almost negligible when compared to water at all Peclet numbers. Experiments are also performed on a diesel engine to assess the effect of nanofluids on its emission characteristics. The investigation shows that using nanofluids resulted in 12.5% reduction of NO<sub>x</sub> emissions at full load and about 3-5% at no load and part load.

**Keywords:** Nanofluid, Heat exchanger, Heat transfer, NO<sub>x</sub> emissions

Cooling is one of the most important technical challenges which is being faced by numerous industries such as automobile, electronics and manufacturing. New technological developments are increasing thermal loads and require faster cooling. The conventional single phase methods in increasing the cooling rate (fins and microchannels) have already been utilized to their maximum potential. Hence, there is an urgent need for new and innovative coolants to achieve high performance cooling<sup>1,2</sup>. Thermal conductivities of traditional heat transfer fluids, such as engine coolants, lubricants and water are very low. With increasing global competition, industries had felt a strong need to develop energy efficient heat transfer fluids with significantly higher thermal conductivities than currently available fluids. The new coolants with their higher thermal performance will reduce the overall size of heat exchanger/radiator and may increase vehicle fuel efficiency.

Nanofluids are made by suspending nanoparticle of materials such as C, Cu, or CuO in liquids such as oil, water and engine coolant. They are heat transfer fluids containing suspended nanoparticles, which have been

developed to meet highly demanding cooling challenges. Nanofluids are a new class of solid-liquid suspensions consisting of nanometer sized (<100 nm) solid particles suspended in heat transfer fluids such as water, ethylene and propylene glycol. The improvement of lubricity of engine oil by adding nanoparticles was investigated by Kao *et al.*<sup>3</sup>

Choi *et al.*<sup>4</sup> showed that nanofluids have the potential to be the next generation of coolants for vehicle thermal management due to their significantly higher thermal conductivities. Several researchers<sup>5-9</sup> showed that the convective heat transfer coefficient increases substantially for nanofluids. This is of great commercial significance, since the heat rejection requirements of automobiles and trucks are continually increasing due to the market trend of employing more powerful engines.

Heat transfer directly affects engine performance, fuel efficiency, materials selection and emissions. The heat generated during combustion should be controlled to maximize engine life and efficiency. In the current scenario of increased emphasis on climate change, improved thermal management systems are required for vehicles, with more compact heat exchangers, innovative heat transfer schemes and environmentally friendly fluids having improved heat

\*Corresponding author (E-mail: raaj.nml@gmail.com)

transfer properties. The benefits of improved heat exchangers and heat transfer devices using nanofluids are reduced weight and smaller components, which take up less room under the hood and it allows for a greater latitude in aerodynamic styling; more effective cooling and increased component life.

Shell-and-tube heat exchangers are commonly used in petrochemical and energy industries due to their relatively simple manufacture and adaptability to different operating conditions. The capital and operating costs of any heat exchanger system are influenced by the pressure drop and heat transfer, which are interdependent parameters. The design and optimization of shell-and-tube heat exchangers include thermodynamic and fluid dynamic considerations, strength calculations, cost estimation and represents a complex process necessitating an integrated approach of design rules, calculation methods and empirical knowledge of various fields<sup>10</sup>. In the past few years several attempts have been made to improve the thermal effectiveness of shell-and-tube heat exchangers. New types of tube-side turbulence promoters (e.g. tube inserts, corrugated tubes) and tube supports (e.g. helical baffles) have been introduced with successful results. Thome *et al.*<sup>11</sup> put forward that the proper application of tubular heat transfer augmentations will be able to reduce heat exchanger tubing linear footage by 25-75% compared to conventional plain tube units. Hosseini *et al.*<sup>12</sup> experimentally investigated the effect of different types of external tube surfaces on shell-side heat transfer coefficient and pressure drop of a shell-and-tube heat exchanger.

Utilizing nanofluids because of the benefits described above, this study focuses on evaluating the performance of shell and tube heat exchanger with nanofluids as the coolant on diesel engine. It also focuses on NO<sub>x</sub> emission from diesel engine when nanofluid used a coolant.

The objective of the present study is to investigate on the heat transfer characteristics, pressure drop and NO<sub>x</sub> of Al<sub>2</sub>O<sub>3</sub>/water nanofluid with various concentrations under laminar flow in shell and tube heat exchanger connected with diesel engine at various load conditions.

### Characterization of Nanoparticles and Nanofluid

Nanocrystalline alumina (Al<sub>2</sub>O<sub>3</sub>) powder (Stock number 44931) was purchased from Alfa Aesar (USA). The X-ray diffraction spectrum of the powder

sample is shown in Fig. 1. The powder XRD was carried out with a Rigaku X-ray diffractometer by Cu-ka<sub>1</sub> radiation in the range of 20-80°. All the reflections in the XRD pattern can be indexed to the tetragonal phase of Al<sub>2</sub>O<sub>3</sub> using Joint Committee on Powder Diffraction Standards (JCPDS). The average grain size of the dry powder is calculated to be 40.3 nm using the Sherrer formula.

Nanofluids with a required volume concentration of 0.5%, 1%, 1.5% and 2% were then prepared by dispersing the specified amount of Al<sub>2</sub>O<sub>3</sub> nanoparticles in water by using an ultrasonic vibrator (Toshiba, India) generating ultrasonic pulses of 100 W at 36 ± 3 kHz. To get a uniform dispersion and stable suspension which determine the final properties of nanofluids, the nanofluids were kept under ultrasonic vibration continuously for 6 h<sup>13</sup>. No surfactant or pH manipulators were used, as they may have some influence on the effective thermal conductivity of nanofluids<sup>14</sup>. The pH of the prepared nanofluids were measured by a pH meter (Cyber pH-14L) and found to be around 4.8 which is far from the isoelectric point of 9.2 for alumina nanoparticles<sup>15</sup>. This ensured that the nanoparticles were well dispersed and the nanofluid was stable because of very large repulsive forces among the nanoparticles when pH is far from isoelectric point. Thus, the Al<sub>2</sub>O<sub>3</sub>/water nanofluids prepared in the present work were found to be very stable for several weeks without visually observable sedimentation.

### Experimental Procedure

A schematic diagram of the experimental set-up used to investigate heat transfer enhancement of nanofluid in shell and tube heat exchanger used in a diesel engine is shown in Fig. 2. It consists of two flow loops, one for Al<sub>2</sub>O<sub>3</sub> nanofluid (i.e. tube loop,

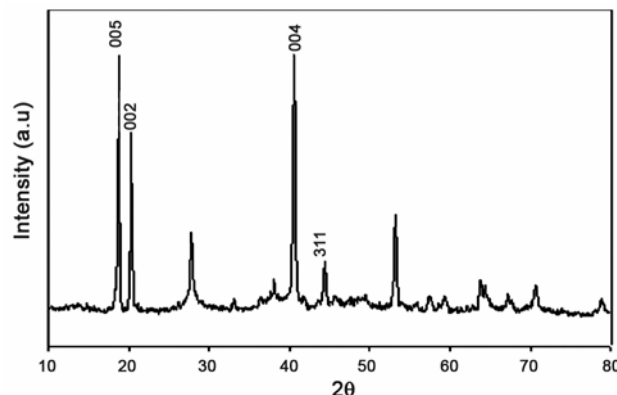


Fig. 1—XRD of Al<sub>2</sub>O<sub>3</sub> nanoparticles

dotted line), and the other for water (i.e. shell loop, continuous line). Each flow loop consists of a pump with flow meter and a reservoir. The shell and tube heat exchanger consists of 27 copper tubes. The outer and inner diameter of each tube is 13.3 mm and 10 mm respectively. The length of each tube is 8100 mm. All tubes were enclosed within a shell of inner diameter 146 mm. To reduce the heat loss, the heat exchanger and pipelines are insulated with asbestos.

Four K-type standalone thermocouples with a range of 0-140°C are inserted into the inlets and outlets of the shell and tubes in the heat exchanger. They were calibrated with PT100 type thermocouple. Thermocouples  $T_{ni}$  and  $T_{no}$  measure the nanofluid temperature at the inlet and outlet of heat exchanger tube side while  $T_{wi}$  and  $T_{wo}$  measures the temperature of the water at inlet and outlet of shellside. Flow meters are used in both loops to measure the flow and valves are used to control the flow of the fluids. The flowmeters were calibrated by weighing the collected liquids.

A differential pressure transducer (SGM srl, Italy) able to read up to 10 mm of water is mounted across the tube bundle to measure the pressure drop. A shell and tube heat exchanger with nanofluid was used to cool a single cylinder four stroke diesel engine (Kirloskar 5HP), which was loaded by an Eddy current Dynamometer.

Experimental uncertainty was calculated using Kline and McClintock<sup>16</sup>. While carrying out the error analysis, probable uncertainties involved in the measurement of various parameters are taken into consideration. Error analysis was carried out by considering the probable uncertainties involved in the measurements. The calculations pointed out that the uncertainties involved in the measurements are around  $\pm 3.8\%$  and  $\pm 8\%$  for overall heat transfer coefficient and Peclet number respectively.

The engine was allowed to run for some time until the system attained steady state. The shell side fluid is then passed into the engine cooling jacket, which absorbs the heat produced due to combustion. Cold fluid, which is water, is allowed into the shell side to transfer the heat from tube side fluid. The four temperatures were noted after the system reaches steady state. First the distilled water is used as tube side fluid and water for shell side. Then,  $\text{Al}_2\text{O}_3/\text{water}$  nanofluid is used in the tube side and water in the shell side. AVL exhaust gas analyzer is used to measure the emissions from the engine.

Prior to each experiment the flow rates of the two streams were adjusted and, after a steady state was established, the data was recorded. Then, the cooling liquid flow rate is then increased and new data was recorded. The above procedure was repeated for various hot water flow rates.

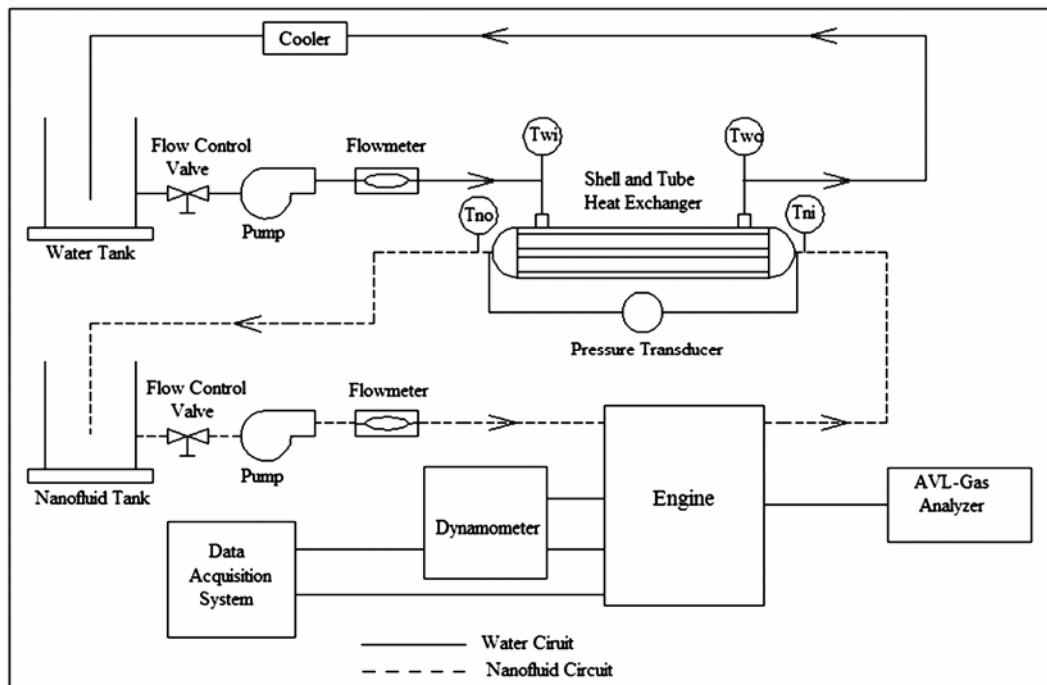


Fig. 2—Schematic diagram of experimental set-up

### Data Reduction

The viscosity and thermal conductivity of nanofluids for various concentrations were measured using Brookfield viscometer (Dv-1 Prime) and KD<sub>2</sub>pro respectively. Both instruments were calibrated before measurements.

Heat transfer rate from hot fluid to cold fluid can be easily calculated from the measured temperature change, flow rate and the specific heat of a fluid.

$$Q_n = m_n C_n (T_{no} - T_{ni}) = Q_w \quad \dots(1)$$

Where  $Q_w$  and  $Q_n$  are the heat transfer rates of water and nanofluid,  $m_n$  is the mass flow rate of water,  $C_n$  is the heat capacity of nanofluid,  $T_{ni}$  and  $T_{no}$  are the temperatures of nanofluid inlet and exit of the tube side of the heat exchanger.

The overall heat transfer coefficient ( $U$ ) is related with a log mean temperature difference (LMTD), of the overall heat transfer coefficient and heat transfer area, which can be expressed as the following equation:

$$Q = UA \Delta T_{LMTD} \quad \dots(2)$$

Where, the definition of a log mean temperature difference is shown in the following equation.

$$\Delta T_{LMTD} = \frac{(T_{ni} - T_{wo}) - (T_{ni} - T_{wi})}{\ln \frac{(T_{ni} - T_{wo})}{(T_{ni} - T_{wi})}} \quad \dots(3)$$

It can be transformed to the overall heat transfer coefficient of fluid in the tube as follows:

$$\frac{1}{U_i} = \frac{1}{h_i} + \frac{D_i L_n \cdot \frac{Do}{Di}}{2K_w} + \left(\frac{Di}{Do}\right) \cdot \left(\frac{1}{ho}\right) \quad \dots(4)$$

Where,  $D_i$  and  $D_o$  are the inside and outside diameter of tube,  $U_i$  is the overall heat transfer coefficient based on inside tube area,  $h_i$  and  $h_o$  are the individual convective heat transfer coefficients of fluids inside and outside the tubes respectively.  $k_w$  is the thermal conductivity of the tube wall.

$$Re = \frac{4m}{\pi D \mu} \text{ and } Pr = \frac{C \mu}{K} \quad \dots(5)$$

Where  $Re$  is Reynolds number and  $Pr$  is the Prandtl number.

The outside heat transfer coefficient can be computed by Bell's procedure<sup>17</sup>.

### Results and Discussion

A number of experiments were conducted to measure the overall heat transfer coefficients of nanofluids that consisted of nano sized alumina particles and water as base fluid. The differences in heat transfer rates of two fluids in both sides of the heat exchanger were very small. The results indicate that there was only a little energy loss in the shell and tube heat exchanger system.

#### Effect on convective heat transfer, pressure drop and NO<sub>x</sub> emission

Figures 3-5 show the relationship between the overall heat transfer coefficient of Al<sub>2</sub>O<sub>3</sub>/water and Peclet number for various volume concentrations. From the results it was understood that there is significant enhancement in overall heat transfer

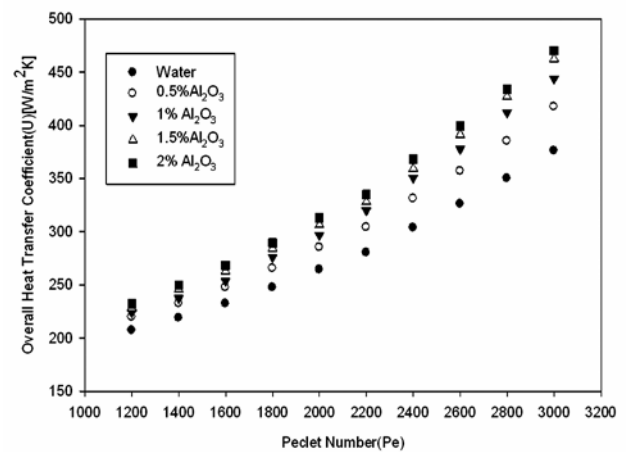


Fig. 3—Overall heat transfer coefficient of Al<sub>2</sub>O<sub>3</sub>/water nanofluid versus Peclet number for various volume concentrations at no load

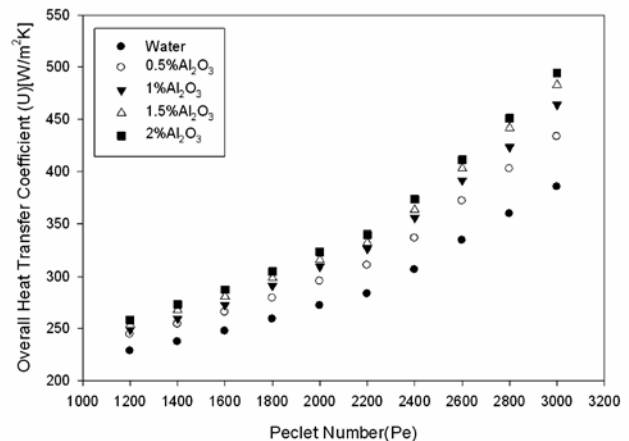


Fig. 4—Overall heat transfer coefficient of Al<sub>2</sub>O<sub>3</sub>/water nanofluid versus Peclet number for various volume concentrations at part load

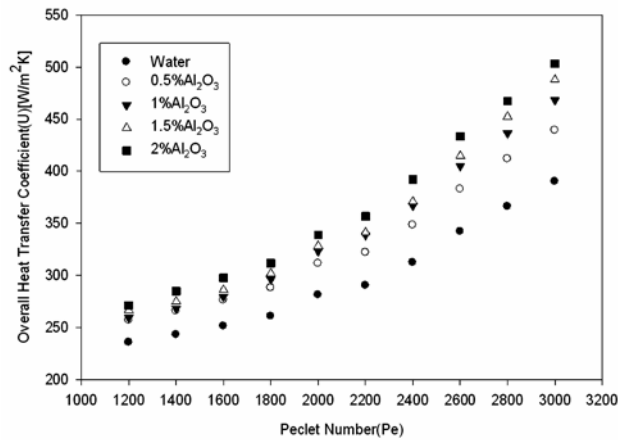


Fig. 5—Overall heat transfer coefficient of  $\text{Al}_2\text{O}_3$ /water nanofluid versus Peclet number for various volume concentrations at full load

coefficient with the base fluid at particular Peclet number. From the graph it was observed that the overall heat transfer coefficient of  $\text{Al}_2\text{O}_3$  nanofluid increases with volume concentration. The maximum overall heat transfer coefficient was observed for 2% volume concentration which is about 25%. For Peclet number 3000, the enhancement at 0.5%, 1%, 1.5% and 2% nanoparticle volume concentrations are about 11%, 18%, 23% and 25%, respectively. From this it is clearly shown that the four fold addition (i.e. 2% nanoparticle) gives only two fold increase (i.e. 25%) in heat transfer coefficient. This may be at higher concentration, agglomeration of nanoparticles suppress the heat transfer characteristics of nanofluid. It was also observed that the enhancement of heat transfer coefficient at lower Peclet number was lower when compared with higher Peclet number. The enhanced heat transfer performance due to the addition of nanoparticles into the working fluid is due to a number of factors. They increase the surface area of the working fluid. They improve the thermal conductivity of the working fluid. There are more collisions and interactions between the working fluid, the particles, and the flow passages. They cause more disorder, integration within the working fluid and the lubricating performance of coolant was enhanced.

The tube side pressure drops along with Peclet number is presented in Fig. 6. From Fig. 6 it was observed that pressure drop increases with the Peclet number and the pressure drop of nanofluids was not significantly high when compared with water. The tube side pressure drop was 7 mm of mercury for water and 7.5 mm of mercury for 2%  $\text{Al}_2\text{O}_3$  of nanofluid at Peclet number of 1200. The pressure drop increased by about 8.5%, when Peclet number

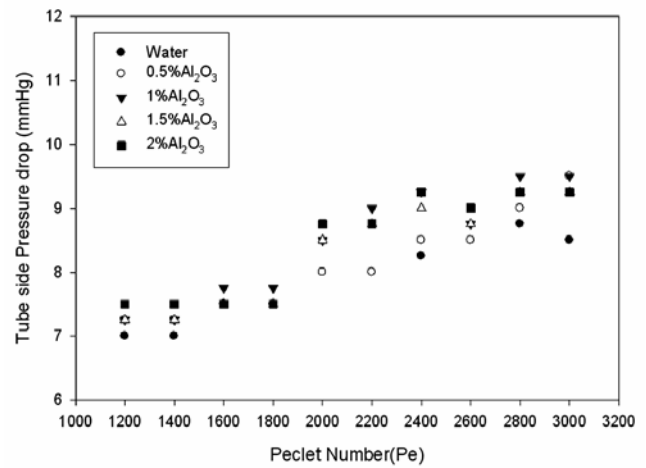


Fig. 6—Pressure drop of  $\text{Al}_2\text{O}_3$ /water nanofluid versus Peclet number for various volume concentrations at full load

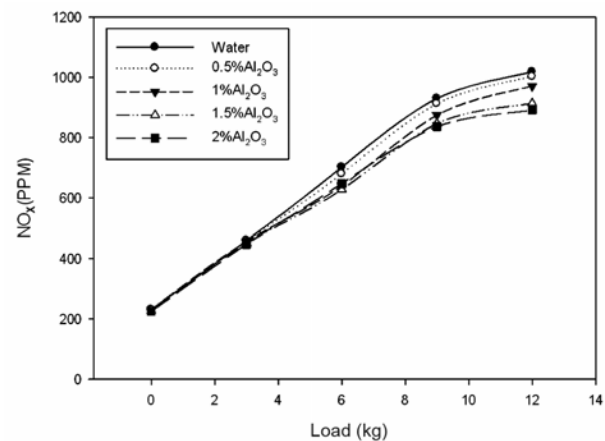


Fig. 7— $\text{NO}_x$  emission versus load for various volume concentrations  $\text{Al}_2\text{O}_3$ /water nanofluid

increased by 3000. The pressure drop caused by the frictional resistance of nanofluid was not appreciable when compared with enhancement in heat transfer.

The factors which governs pressure drop through a heat exchanger pipes are flow rate, density and viscosity. The flow rate has linear relationship with pressure drop. For a particular flow rate the pressure drop of water was lower and it was increased for nanofluid with increased concentration. Since the density of nanofluid at a particular concentration is constant, the dispersing behaviour in pressure drop of nanofluid may be due to viscosity which is mainly influenced by the formation of particle cluster and defragmentation of the cluster.

$\text{NO}_x$  emissions from diesel engines have been shown to be sensitive to engine operating temperature, which is directly related to the level of cooling capacity applied to the engine. Figure 7

presents the  $\text{NO}_x$  emission from the engine for various volume fractions versus different loading conditions. From Fig. 7 it was observed that the  $\text{NO}_x$  emission significantly reduced about 12.5% for 2%  $\text{Al}_2\text{O}_3$ /water nanofluid compared to water at full load of the engine. The  $\text{NO}_x$  emission reduction at no load and part load after the application of 2%  $\text{Al}_2\text{O}_3$ /water nanofluid were about 3% to 5%.

At higher load, it is obvious that  $\text{NO}_x$  emission will be more due to higher combustion temperature. The excess temperature is observed well by the nanofluid which yields the reduction of  $\text{NO}_x$  emission. At full load condition it reduced the emission about 12.5% with no penalty of power reduction.

### Conclusions

Experimental investigations on convective heat transfer and pressure drop characteristics of  $\text{Al}_2\text{O}_3$ /water nanofluid was carried out in the shell and tube heat exchanger.  $\text{Al}_2\text{O}_3$  nanoparticles of 40.3 nm size were used to prepare nanofluid. Following observations were made from the investigation:

- (i)  $\text{Al}_2\text{O}_3$ /water nanofluid having a volume concentration of 0.5% increased the overall heat transfer coefficient by 11% at Peclet number 3000 under no load condition compared to that of distilled water.
- (ii) Further enhancements in overall heat transfer coefficient was observed when  $\text{Al}_2\text{O}_3$ /water nanofluid with higher volume concentration. Overall heat transfer coefficient was increased by 18%, 23% and 25% for  $\text{Al}_2\text{O}_3$ /water nanofluid with volume concentration of 1%, 1.5% and 2% respectively at  $Pe = 3000$  compared to those of distilled water at no load.
- (iii) Overall heat transfer coefficient was increased by 20.5%, 25.4% and 28.4% for  $\text{Al}_2\text{O}_3$ /water nanofluid with volume concentration of 1%, 1.5% and 2% respectively at  $Pe = 3000$  compared to those of distilled water at part load.
- (iv) Overall heat transfer coefficient was increased by 20%, 25% and 29% for  $\text{Al}_2\text{O}_3$ /water nanofluid with volume concentration of 1%, 1.5% and 2% respectively at  $Pe = 3000$  compared to those of distilled water at full load.
- (v) Compared to the pressure drop with distilled water, there was about 0.5-1.5 mm of mercury for a Peclet number of 1200 and 3000.
- (vii)  $\text{NO}_x$  emission from the engine was reduced to 12.5% at full load for nanofluid compared with distilled water.

From the above characteristics  $\text{Al}_2\text{O}_3$ /water nanofluid is better for engine cooling systems due to their capability to respond quickly to temperature changes allowing for the dissipation of more heat, using less coolant, in a shorter period of time.

### Nomenclature

$A$	=	heat transfer area ( $\text{m}^2$ )
$C$	=	specific heat ( $\text{kJ kg}^{-1}\text{K}^{-1}$ )
$D$	=	diameter at the section (tube or shell) (m)
$Pe$	=	Peclet Number
$Pr$	=	Prandtl number (Dimensionless)
$Q$	=	heat transfer rate (kW)
$Re$	=	Reynolds number (Dimensionless)
STHE	=	Shell and Tube heat exchanger
$U$	=	overall heat transfer coefficient ( $\text{Wm}^{-2}\text{K}^{-1}$ )
$T$	=	temperature ( $^{\circ}\text{C}$ )
$\Delta T_{\text{LMTD}}$	=	logarithmic mean temperature difference (K)
$d$	=	grain size
$h$	=	heat Transfer Coefficient ( $\text{Wm}^{-2}\text{K}^{-1}$ )
$k$	=	thermal conductivity ( $\text{Wm}^{-1}\text{K}^{-1}$ )
$m$	=	mass flow rate (kg/s)

### Greek Symbols

$\mu$	=	dynamic viscosity ( $\text{N-s/m}^2$ )
$\nu$	=	kinematic viscosity ( $\text{m}^2/\text{s}$ )

### Subscripts

$s$	=	shell
$t$	=	tube
$ni$	=	nanofluid inlet
$no$	=	nanofluid outlet
$n$	=	nanofluid
$w$	=	water
$wi$	=	water inlet
$wo$	=	water outlet

### References

- 1 Phillpot J A, Choi S U S & Keblinski P K, *Ann Rev Mater Res*, 34 (2004) 219-246.
- 2 Choi S U S, Zhang Z G & Keblinski P K, *Nanofluids, Encyclopedia of Nanoscience and Nanotechnology* (American Scientific Publishers) vol. 6 (2004) 757-773.
- 3 Kao M J, Tsung H & Lin H M, *J Phys: Conf Ser*, 48 (2006) 663-666.
- 4 Choi S U S, Yu W, Hull J R, Zhang Z G & Lockwood F E, *SAE 2001-01-1706* (2001), 139-144.
- 5 Li Q & Yimin X, *Science in China (Series E)*, 45 (4) (2002) 408-416.
- 6 Lee S & Choi S U S, *ASME PVP 342/MD 72* (1996) 227-234.
- 7 Yang Y, Zhang Z G, Grulke E A, Anderson W B & Wu G, *Int J Heat Mass Transfer*, 48 (2005) 1107-1116.
- 8 Wen D & Ding Y, *Int J Heat Mass Transfer*, 48 (2004) 5181-5188.
- 9 Ding Y, Alias H, Wen D & Williams R, *Int J Heat Mass Transfer*, 49(2006) 240-250.
- 10 Reppich M & Kohoutek J, *Comput Chem Eng*, 18 (Suppl 1) (1994) S295-S299.
- 11 Thome J R, *J Enhanced Heat Transfer*, 4 (2) (1997) 147-161.

- 12 Hosseini R, Hosseini-Ghaffar A & Soltani M, *Appl Thermal Eng*, 27 (2007) 1001-1008.
- 13 Lee J H, Hwang K S, Jang S P, Lee B H, Kim J H, Choi S U S & Choi C J, *Int J Heat Mass Transfer*, 51 (2008) 2651-2656.
- 14 Das S K, Putra N, Thiesen P & Roetzel W, *J Heat Transfer*, 125(2003) 567-574.
- 15 Xie H, Chen L & Wu Q, *High Temp High Pressures*, 37 (2008) 127-135.
- 16 Holman J P, *Experimental Methods for Engineers*, (Tata McGraw-Hill, India), 2007.
- 17 Farajollahi B, Etemad S Gh & Hojjat M, *Int J Heat Mass Transfer*, 53 (2010) 12-17.